Scalar-field quintessence by cosmic shear: CFHT data analysis and forecasts for DUNE

2007 J. Phys. A: Math. Theor. 40 7105

(http://iopscience.iop.org/1751-8121/40/25/S69)

IOP Publishing Journal of Physics A: Mathematical and Theoretical

J. Phys. A: Math. Theor. **40** (2007) 7105–7112 doi:10.1088/1751-8113/40/25/S69

Scalar-field quintessence by cosmic shear: CFHT data analysis and forecasts for DUNE

C Schimd[1] **and I Tereno**[2,3]

[1] DAPNIA, CEA Saclay, 91191 Gif-sur-Yvette Cedex, France
[2] Argelander-Institut für Astronomie, Universität Bonn, 53121 Bonn, Germany
[3] Institut d'Astrophysique de Paris, 98bis Bvd. Arago, 75014 Paris, France

E-mail: carlo.schimd@cea.fr

Received 31 October 2006, in final form 16 March 2007
Published 6 June 2007
Online at stacks.iop.org/JPhysA/40/7105

Abstract
A light scalar field, minimally or not-minimally coupled to the metric field, is a well-defined candidate for the dark energy, alleviating the fine-tuning problem intrinsic to the cosmological constant and avoiding the difficulties of parameterizations. We present a general description of the weak gravitational lensing valid for every metric theory of gravity, including vector and tensor perturbations for a non-flat spatial metric. Based on this description, we investigate two minimally coupled scalar-field quintessence models using VIRMOS-Descart and CFHTLS cosmic-shear data, and forecast the constraints for the proposed space-borne wide-field imager DUNE.

PACS numbers: 98.80.−k, 98.80.Jk, 98.62.Sb, 95.36.+x

(Some figures in this article are in colour only in the electronic version)

1. Introduction

There is overwhelming evidence that the description of the observed universe cannot rely only on the assumption of the Copernican principle, on the general relativity and on the Standard Model of particle physics, eventually extended to include a dark matter candidate [1]. We shall define *dark energy* as anything which represents the failure of some of these assumptions: (i) it could be a signature of the dynamical effect of inhomogeneities, not properly averaged when accounting for the background dynamics [2]. (ii) Gravitational interactions (on cosmological scales) could be not described by the Hilbert–Einstein action, requiring, e.g., the inclusion of higher order terms as in scalar–tensor theories of gravity [3] or a formulation in more than four dimensions, as in braneworld scenarios or superstring theories [4]. (iii) Dark energy is an effective 'matter' field, often dubbed quintessence [5], not clustering on the observed scales and possibly coupled to the matter fields [6], provided the weak equivalence principle is preserved.

A combination of these options is the last possibility, like in extended quintessence scenarios [7]. One can therefore define *classes* of models, characterized by definite observational and experimental signatures [8].

The weak gravitational lensing by large-scale structures, or *cosmic shear*, is a geometrical observable which depends on both background evolution and structures formation [9]. Therefore, it is a promising tool to investigate dark energy, allowing one to explore in unbiased way the low-redshift universe where dark energy mostly acts [10, 11]. Cosmic shear has been exploited to investigate ordinary quintessence scenarios, considering a parameterization of the quintessence equation of state [10–12]. Based on [13] and following [14], we use a general formulation of weak lensing valid for every metric theory of gravity, thus for general relativity and scalar–tensor theories as well [15] (see also [16] for an alternative approach). We therefore move towards 'physics'-inspired models, for the first time using cosmic-shear real data by CFHT surveys and evaluating the performance of a space-based wide-field survey [17].

2. Geometry of null congruences: cosmic shear

Every galaxy defines a light bundle, or congruence of null geodesics $x^\mu(\lambda) = \bar{x}^\mu(\lambda) + \xi^\mu(\lambda)$ deviating from a fiducial, arbitrary geodesic $\bar{x}^\mu$ by a displacement ξ^μ, converging at the observer position O (where $\xi^\mu = 0$), and whose tangent vectors $k^\mu \equiv \mathrm{d}x^\mu/\mathrm{d}\lambda$ are solution of $k_\mu k^\mu = 0$ and $k^\nu \nabla_\nu k^\mu = 0$ (we take the affine parameter λ vanishing in O and increasing towards the past). The shape of the light bundle is described by a deformation tensor $\mathcal{D}^a_b$, whose evolution along the fiducial geodesic (defined by $\bar{k}^\mu$) is deduced from the geodesic deviation equation for ξ^μ. Setting $\xi_a(\lambda) = n^a_\mu \xi^\mu(\lambda) \equiv \mathcal{D}^b_a(\lambda)\dot{\xi}_b(0)$, on the plane $\{n^\mu_1, n^\mu_2\}$ orthogonal to the line-of-sight $\left(n^a_\mu n^\mu_b = \delta^a_b, n^a_\mu \bar{k}^\mu = 0\right)$ we have

$$\ddot{\mathcal{D}}^a_b = \mathcal{R}^a_c \mathcal{D}^c_b \tag{1}$$

with initial conditions $\mathcal{D}^a_b(0) = 0$, $\dot{\mathcal{D}}^a_b(0) = \delta^a_b$, the dot referring to a derivation with respect to λ. Here, $\mathcal{R}^a_b \equiv R^\alpha_{\mu\nu\beta}\bar{k}^\mu\bar{k}^\nu n^\alpha_a n^\beta_b = -\frac{1}{2}R_{\mu\nu}\bar{k}^\mu\bar{k}^\nu\delta^a_b + C^\alpha_{\mu\nu\beta}\bar{k}^\mu\bar{k}^\nu n^a_\alpha n^\beta_b$ is the optical tidal matrix written in terms of the Riemann tensor $R^\alpha_{\mu\nu\beta}$ or in terms of the Ricci and Weyl tensors, respectively, $R_{\mu\nu}$ and $C^\alpha_{\mu\nu\beta}$. This latter expression highlights the sources of the isotropic and anisotropic deformation of the original image, see [18]. See also [19] for a description of the characteristic fingerprint distortion field of the Weyl tensor.

As long as the spacetime is described by a background metric with small perturbations $h_{\mu\nu}$, equation (1) is solved order-by-order in $h_{\mu\nu}$. We shall consider with Robertson–Walker metric $g^{\mathrm{RW}}_{\mu\nu}$ with scalar, vector and tensor perturbations,

$$g_{\mu\nu}\,\mathrm{d}x^\mu\,\mathrm{d}x^\nu = a^2(\eta)\{-(1-2\phi)\,\mathrm{d}\eta^2 + 2B_i\,\mathrm{d}\eta\,\mathrm{d}x^i + [(1+2\psi)\gamma_{ij} + 2E_{ij}]\,\mathrm{d}x^i\,\mathrm{d}x^j\}, \tag{2}$$

with $\nabla^i B_i = \nabla^i E_{ij} = E^i_i = 0$. The spatial metric $\gamma_{ij}\,\mathrm{d}x^i\,\mathrm{d}x^j = \mathrm{d}\chi^2 + S^2_K(\chi)\,\mathrm{d}\Omega^2$ is written in terms of the comoving angular-diameter distance $S_K(\chi) = \sin(\sqrt{K}\chi)/\sqrt{K}$ allowing for curvature $K = \{-1, 0, 1\}$, χ is the comoving radial distance and $\mathrm{d}\Omega^2$ is the infinitesimal solid angle. Exploiting the conformal invariance of null geodesics, for $\bar{g}^{\mathrm{RW}}_{\mu\nu} \equiv a^{-2}(\eta)g^{\mathrm{RW}}_{\mu\nu}$, the optical tidal matrix at zeroth and first orders reads

$$\mathcal{R}^{a(0)}_b = -K\delta^a_b, \qquad \mathcal{R}^{a(1)}_b = D^a D_b(\phi + \psi + B_{\hat{\chi}} + E_{\hat{\chi}\hat{\chi}}) + K\left(E^a_b - E_{\hat{\chi}\hat{\chi}}\delta^a_b\right), \tag{3}$$

with D_a being the covariant derivative with respect to the spatial metric γ_{ij} and $\hat{\chi}$ denoting the component along the line-of-sight. Accordingly, equation (1) leads to

$$\ddot{\mathcal{D}}^{(0)} = -K\mathcal{D}^{(0)}, \qquad \ddot{\mathcal{D}}^{(1)} = -K\mathcal{D}^{(1)} + \mathcal{R}^{(1)}\mathcal{D}^{(0)}. \tag{4}$$

Integrating over $\mathrm{d}\lambda = \mathrm{d}\chi$ and finally rescaling the solution $\mathcal{D} = \mathcal{D}^{(0)} + \mathcal{D}^{(1)}$ by the (angular) distance of the source galaxy, $d_{\mathrm{A}}(\lambda)$, we get the amplification matrix $\mathcal{A}_{ab} = \mathcal{D}_{ab}(\lambda)/d_{\mathrm{A}}(\lambda)$; its

diagonal and off-diagonal terms, which account for the isotropic and anisotropic deformation of the original image, are the observed quantities. In particular, neglecting vector and tensor perturbations, from $\mathcal{R}_b^{a(1)} \equiv D^a D_b \Phi$, the convergence field $\kappa = \left(1 - \frac{1}{2}\,\mathrm{Tr}\,\mathcal{A}\right)$ induced by a sources located at $(S_K(\chi)\boldsymbol{\theta}, \chi)$ reads

$$\kappa(\boldsymbol{\theta}, \chi) = \int_0^{\chi} \mathrm{d}\chi' \frac{S_K(\chi')S_K(\chi' - \chi)}{S_K(\chi)} \Delta_2 \Phi[S_K(\chi')\boldsymbol{\theta}, \chi'] \tag{5}$$

where the deflecting potential Φ is calculated solving the field (e.g. Einstein) equations. Eventually, one has to integrate over the distribution of sources $n(\chi)$ along the line-of-sight. Usually, a fitting function of the form $n(z) \propto (z/z_{\mathrm{s}})^{\alpha} \exp[-(z/z_{\mathrm{s}})^{\beta}]$ is taken to reproduce the observed distribution of sources as a function of redshift z.

In order to extract the cosmological signal getting rid of the intrinsic ellipticity of sources, one measures n-point correlation functions. Restricting ourselves to two-point ones, in the flat sky approximation, the convergence and shear power spectra are

$$P_\kappa(\ell) = P_\gamma(\ell) = \frac{1}{4} \int \mathrm{d}\chi\, g^2(\chi)[k^4 P_\Phi(k, \chi)]_{k=\ell/S_K(\chi)} \tag{6}$$

where $g(\chi) = \int_\chi^{\chi_{\mathrm{H}}} \mathrm{d}\chi'\, n(\chi') S_K(\chi' - \chi)/S_K(\chi')$ and P_Φ is the three-dimensional power spectrum of the deflecting potential. Two-point correlation functions in the real space, like top-hat shear or aperture mass variances, are filtered integrals of this quantity [9].

3. Quintessence by cosmic shear: parameterizations versus 'physical' models

The use of parameterizations for the quintessence equation of state generally assumes a Friedmann–Robertson–Walker universe, thus excluding *a priori* other options for the dark-energy sector. Moreover, every parameterization is affected by the choice of a dataset-dependent pivot redshift [10], by the consistency with a model for the speed of sound determining the formation of structures, and by the large number of parameters required to suitably account for a 'realistic' dynamics over a wide range of redshift [20]. Dealing with 'physics'-inspired models one would overcome these problems, aiming to investigate if a class of theory is compatible with observations at low and high redshifts.

We explore two ordinary quintessence scenarios, realized by a self-interacting scalar degree of freedom Q with Ratra–Peebles (RP) and supergravity (SUGRA) potentials

$$V_{\mathrm{RP}}(Q) = M^{4+\alpha}/Q^{\alpha}; \qquad V_{\mathrm{SUGRA}}(Q) = M^{4+\alpha} \exp\left(Q^2/2M_{\mathrm{Pl}}^2\right)/Q^{\alpha} \tag{7}$$

which guarantee the (partial) solution of the fine-tuning problem [7]. The mass scale M is uniquely determined once α and the density parameter Ω_{Q} are fixed.

Background and perturbations evolution in linear regime are computed solving the Einstein and Klein–Gordon equations by means of a Boltzmann code described in [21]. Dealing with general relativity, on sub-horizon scales one can safely use the Poisson equation to relate the deflecting potential $P_\Phi = 4P_\phi$ to the power spectrum of matter perturbations. In order to account for the nonlinear matter power spectrum in a feasible way for a grid-based likelihood analysis, we use two linear-to-nonlinear mappings [23] (see [15] for a generalization in scalar–tensor theories). Although calibrated on ΛCDM N-body simulations, we suppose that they holds for QCDM models, provided the linear regime is properly taken into account using the correct linear growth factor and the spectra normalized to high redshift (by CMB). Indeed, the Q-field mostly acts on the background dynamics affecting the onset of the nonlinear regime, while the successive evolution on small scales (affecting the structure of single galaxies/halos, bias, etc) is essentially dictated by astrophysical processes. See however [24], where the effects of the QCDM background dynamics on structure formation have been scrutinized.

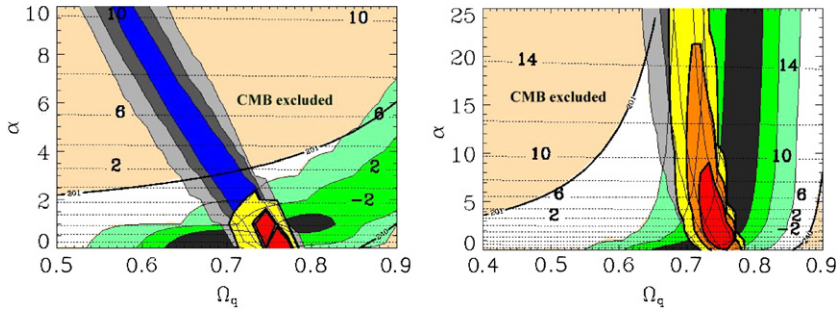

Figure 1. Likelihood analysis of the quintessence parameter space for RP (left) and SUGRA (right) models, marginalizing over (n_s, z_s), using CFHT cosmic-shear data (blue contours, at 68, 95 and 99%), the 'goldset' of SnIa (green) and both jointly (red). The shaded region is excluded by the location of the first peak of CMB-$C_\ell^{\rm TT}$, according to WMAP-3yr data (see the text for details). Dotted lines refer to $\log_{10} M/$ GeV, see equation (7).

We allow $(\Omega_{\rm Q}, \alpha, n_s, z_s)$ to vary, keeping the other parameters fixed, see [17] for details. Furthermore, we marginally use CMB data to reduce the quintessence parameter space, see the next section.

4. Joint cosmic-shear–SnIa data analysis

We combined VIRMOS-Descart, CFHTLS-deep and CFHTLS-wide/22 deg^2 top-hat shear variance data (see [12, 17] for details) to investigate the sensitivity to the description of the nonlinear regime. The results look different when using the Peacock and Dodds or the Smith *et al* prescriptions [23], which are based on different modelling of the nonlinear clustering. Note that both mappings do not include the effects of baryons, not negligible on the scales of interest to cosmic shear [25]. Interestingly, the quintessence parameter space $(\Omega_{\rm Q}, \alpha)$ seems not to be sensitive to nonlinear gravitational clustering, probing that (ordinary) quintessence primarily acts on geometry.

Combining the cosmic-shear data with the 'goldset' of supernovae Ia (SnIa) [27] and marginalizing over n_s and z_s, figure 1, one can safely constraint RP models ($\alpha < 1, \Omega_{\rm Q} = 0.75^{+0.03}_{-0.04}$ at 95%) because of the strong degeneracy between the two observables. More care is needed for SUGRA models, where the superposition of likelihood contours is severely dependent on reliability of their location, ultimately dependent on systematics. As for cosmic-shear measurements, redshift and shear calibration of datasets are the crucial points [26]. If we trust in current control of systematics, we have $\alpha = 2^{+18}_{-2}, \Omega_{\rm Q} = 0.74^{+0.03}_{-0.05}$ at 95%. SUGRA models appear less constrained than RP ones because of the milder dependence of their low-redshift dynamics on α, see [17] for more details. Eventually, one can extract the value of the mass scale M, whose contours follow the estimate $\log_{10}(M/{\rm GeV}) \simeq (19\alpha - 47 + \log\Omega_{\rm Q})/(\alpha + 4)$ which holds as long as $Q \sim M_{\rm Pl}$.

Exploiting the one-to-one relation between $(\Omega_{\rm Q}, \alpha)$ and the values of the quintessence equation of state and its time derivatives (valid for $\alpha \neq 0$) at whatever redshift, we translate the likelihood contours of the joint analysis in a (w, w') parameter space ($w' \equiv {\rm d}w/{\rm d}\ln a$), evaluated at $z = 0$, see figure 2. This is useful to compare the models at hand with other classes of models [28], and with the dynamical constraints $w' > -3(1 - w^2)$ (solid line), corresponding to a Q-field's speed of sound $c_{\rm s}^2 < 1$, and $3w(1 + w) < w' < 0.2w(1 + w)$ (dashed line), characterizing the so-called freezing models. For every set of points

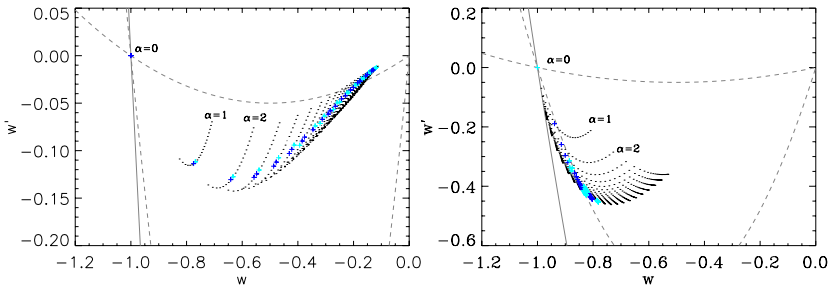

Figure 2. Likelihood analysis of the quintessence parameter space (Ω_Q, α) transposed in the (w, w') parameter space (at $z = 0$), for RP (left) and SUGRA (right) models, using only the combined cosmic-shear datasets. Dark and light crosses refer to points lying, respectively, within the 68% and 95% confidence levels of the original likelihood, while dots correspond to remaining points of the (Ω_Q, α) grid (see section 4).

characterized by the same α (linearly varying by $\Delta\alpha = 1$), points span the Ω_Q range [0.4, 0.9] from top to bottom (linear steps $\Delta\Omega_Q = 0.025$). The fact that w' is larger for SUGRA models indicates that the low-redshift dynamics is faster than in RP case; this is due to the fact that, for every α, all the SUGRA models converge to a narrow range of w values at $z = 0$. The (w, w') representation is also helpful to explain the region of the quintessence parameter space excluded by the location of the first peak ℓ_{1st} of CMB temperature anisotropies, according to WMAP-3yr data [22] (we considered the very conservative range $201 \lesssim \ell_{1st} \lesssim 240$, see figure 1): models with large values of α have large w, thus a distance to the last-scattering surface larger than a ΛCDM model. Hence, the acoustic horizon is expected at smaller multipoles.

5. Wide surveys: forecasts

Focusing on wide surveys (figure 3), one can investigate angular scales where the contamination of the nonlinear regime is reduced (a residual being always present because of the integration along the line-of-sight, see equation (5)). Using a synthetic realization of the CFHTLS-wide full survey, we performed a likelihood analysis using only angular scales $\gtrsim$20 arcmin. Since it corresponds to cutting off larger wavemodes k, the contours concerning all the cosmological parameters we considered broaden. However, the contours of the quintessence parameter space are less affected by this cut. In particular, SUGRA models seem to be very slightly dependent on α but highly sensitive on Ω_Q. Finally, remark that the results depend on $n(z)$, which we suppose to be the same of that measured for the 22 deg^2 dataset.

This analysis points towards the gain achievable by a very-wide survey, for which the quality image requirements very likely need space-based observations. We thus forecast the improvement on the RP and SUGRA models considering a DUNE-like mission [29], a shallow survey covering 20 000 deg^2. The results depicted in figure 4 illustrate the gain with respect to the full CFHTLS-wide survey. It has to be stressed, however, that this estimation is based on an approximate distribution of sources, assumes a perfect correction of the point spread function and finally is marginalized over a small number of cosmological parameters (which beside $(\Omega_q, \alpha, n_s, z_s)$ include the optical reionization depth τ_{reion}, finally acting on the CMB normalization of the shear spectrum).

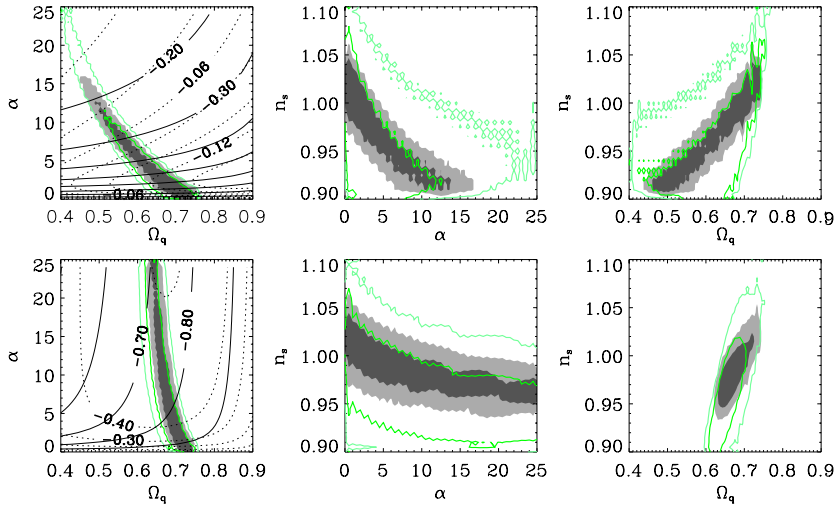

Figure 3. Likelihood analysis of the top-hat shear variance based on a synthetic realization of the 170 deg^2 CFHTLS-wide survey (filled contours; 68% and 95% c.l.) and considering only scales $\gtrsim$20 arcmin (empty contours), for RP (upper) and SUGRA (lower). Solid (dotted) lines in the (Ω_q, α) plane represent the value of w (w') at $z = 0$.

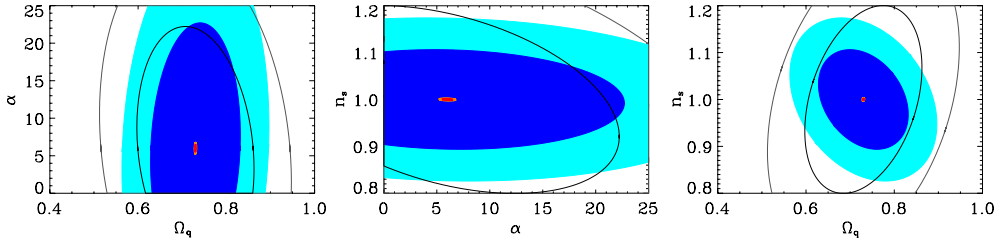

Figure 4. Fisher analysis forecast for a CFHTLS-wide 170 deg^2 survey (wide/blue ellipses) and a DUNE-like 20 000 deg^2 survey (small/red ellipses; contours at 1 and 2σ) for the (Ω_Q, α, n_s) parameter space, marginalizing over $(\tau_{\rm reion}, z_s)$. Filled (empty) contours refer to SUGRA (RP) models both centred at the same fiducial model. For RP, only CFHTLS-wide contours are shown.

6. Concluding remarks

Using a general formulation of weak lensing valid for every metric theory of gravity, thus for general relativity as well as scalar–tensor theories of gravitation, we dispose of tools to study several classes of the dark-energy sector at both low and high redshifts. Notably, we can combine weak-lensing, supernovae and CMB observables avoiding the use of parameterizations, which complicates a safe combination of datasets and can hardly match any well-defined theory. As for cosmic shear, we explicit here the weak-lensing formulation to include vector and tensor perturbations of the metric in a non-flat geometry (equations (3) and (4)), which will be useful, e.g., for joint analysis including the contribution of primordial gravitational waves.

We investigate two classes of ordinary quintessence models by means of real cosmic-shear data, combining with supernovae data, putting forward the interest of using CMB

data to normalize the spectra and thus define the onset of the nonlinear regime of structures formation. We get an upper bound on the slope of the self-interacting potential for RP models, finally compatible with a ΛCDM model, while SUGRA models could be distinguished from the latter provided a good control of systematics is guaranteed. In particular, we obtained $\alpha_{\rm SUGRA} = 2^{+18}_{-2}$, $\Omega_{\rm Q} = 0.74^{+0.03}_{-0.05}$ at 95%, corresponding to a mass scale M for the quintessence potential ranging from ~ 1 meV to $\sim 10^{14}$ GeV. The contamination of nonlinear gravitational clustering, the most delicate issue on the theoretical side, can be reduced when disposing of wide surveys, which reasonably require space-based missions to achieve a high-precision characterization of the dark-energy sector. For a class 10 000 deg^2 survey, a simplistic Fisher-matrix analysis indicates a gain of 10–15 on the quintessence parameter space for the two models we considered.

Acknowledgments

The authors are grateful to Jean-Philippe Uzan, Yannick Mellier, Alexandre Réfrégier and to an anonymous referee for fruitful comments on the manuscript. CS thanks IAP for hospitality.

References

[1] Peebles P J E and Ratra B 2003 *Rev. Mod. Phys.* **75** 559
[2] Ellis G F R and Buchert T 2005 *Phys. Lett.* A **347** 38
Kolb E W, Matarrese S and Riotto A 2006 *New J. Phys.* **8** 322
[3] Damour T and Esposito-Farèse G 1992 *Class. Quantum Grav.* **9** 2093
[4] Brax P and van de Bruck C 2003 *Class. Quantum Grav.* **20** R201
Lidsey J E, Wands D and Copeland E J 2000 *Phys. Rep.* **337** 343
[5] For a review see Copeland E J, Sami M and Tsujikawa S 2006 *Int. J. Mod. Phys.* D **15** 1753
[6] Amendola L 2000 *Phys. Rev.* D **62** 043511
[7] Uzan J P 1999 *Phys. Rev.* D **59** 123510
Chiba T 1999 *Phys. Rev.* D **60** 083508
Perrotta F, Baccigalupi C and Matarrese S 2000 *Phys. Rev.* D **61** 023507
[8] Uzan J-P 2006 *Gen. Rel. Grav.* **39** 307
[9] Mellier Y 1999 *Annu. Rev. Astron. Astrophys.* **37** 127
Bartelmann M and Schneider P 2001 *Phys. Rep.* **340** 291
[10] Hu W and Jain B 2004 *Phys. Rev.* D **70** 043009
[11] Benabed K and van Waerbeke L 2004 *Phys. Rev.* D **70** 123515
[12] Jarvis M *et al* 2006 *Astrophys. J.* **664** 71
Semboloni E *et al* 2006 *Astron. Astrophys.* **452** 51
Hoekstra H *et al* 2006 *Astrophys. J.* **647** 116
[13] Sachs R 1962 *Proc. Roy. Soc.* A **270** 103
[14] Uzan J-P and Bernardeau F 2000 *Phys. Rev.* D **63** 023004
[15] Schimd C, Uzan J-P and Riazuelo A 2005 *Phys. Rev.* D **71** 083512
[16] Acquaviva V, Baccigalupi C and Perrotta F 2004 *Phys. Rev.* D **70** 023515
[17] Schimd C *et al* 2007 *Astron. Astrophys.* **463** 405
[18] Kristian J and Sachs R 1966 *Astrophys. J.* **143** 379
[19] Chrobok T and Perlick V 2001 *Class. Quantum Grav.* **18** 3059
[20] Corasaniti P S and Copeland E J 2003 *Phys. Rev.* D **67** 063521
[21] Riazuelo A and Uzan J-P 2002 *Phys. Rev.* D **66** 023525
[22] Spergel D N *et al* 2007 *Astrophys. J.* at press
[23] Peacock J A and Dodds S J 1996 *Mon. Not. R. Astron. Soc.* **280** L19
Smith R E *et al* 2003 *Mon. Not. R. Astron. Soc.* **341** 1311
[24] Dolag K *et al* 2004 *Astron. Astrophys.* **416** 853
Maio *et al* 2006 *Mon. Not. R. Astron. Soc.* **373** 869

[25] White M 2005 *Astropart. Phys.* **24** 334
Zhan H and Knox L 2004 *Astrophys. J.* **616** L75
[26] van Waerbeke L *et al* 2006 *Astropart. Phys.* **26** 91
[27] Tonry *et al* 2003 *Astrophys. J.* **594** 1
[28] Barger V *et al* 2006 *Phys. Lett.* B **635** 61
Scherrer R J 2006 *Phys. Rev.* D **73** 043502
[29] Réfrégier A *et al* 2006 *Proc. SPIE* **6265** 62651Y (*Preprint* astro-ph/0610062)